Carbohydrate Polymers 115 (2015) 238–245

Contents lists available at ScienceDirect

Carbohydrate Polymers

journal homepage: www.elsevier.com/locate/carbpol

Green chitosan–carbon dots nanocomposite hydrogel film with superior properties

Achyut Konwar[a], Neelam Gogoi[a], Gitanjali Majumdar[b], Devasish Chowdhury[a,*]

[a] Material Nanochemistry Laboratory, Physical Sciences Division, Institute of Advanced Study in Science and Technology, Paschim Boragaon, Garchuk, Guwahati 781035, India
[b] Department of Chemistry, Assam Engineering College, Jalukbari, Guwahati 781013, India

ARTICLE INFO

Article history:
Received 7 July 2014
Received in revised form 13 August 2014
Accepted 15 August 2014
Available online 23 August 2014

Keywords:
Chitosan
Carbon dots
Nanocomposite
Hydrogel
Mechanical properties
Thermal properties

ABSTRACT

In this work we report novel chitosan–carbon dots nanocomposite hydrogel films. A new green source "tea" was used as precursor for carbon dots (CDs). The electrostatic interaction of positive charge on chitosan and negative charge on CDs prepared from tea was used for the successful preparation of a stable and robust chitosan–carbon dots nanocomposite hydrogel film. The hydrogel films were characterized by UV–visible spectroscopy, X-ray diffraction (XRD), Fourier transformed infra-red spectroscopy (FTIR), scanning electron microscope (SEM), fluorescent microscopy, thermogravimetric analysis (TGA) and contact angle analysis. It was observed that chitosan–carbon dots hydrogel films are soft but tough with superior UV–visible blocking, swelling, thermal and mechanical properties in comparison to chitosan hydrogel film. Moreover chitosan–carbon dots films are more water repellent (hydrophobic) as indicated by their high contact angle values. Thus, fabrication of such green soft but tough biocompatible chitosan–carbon dots nanocomposite hydrogel films offers tremendous bio-medical and industrial applications.

1. Introduction

Chitosan, the cationic (1-4)-2-amino-2-deoxy-<beta>-D-glucan partly acetylated to the typical extent close to 0.25, is industrially produced from marine chitin (Muzzarelli, 2010; Muzzarelli, 2012; Muzzarelli et al., 2012). It has attracted attention owing to its superior features such as biocompatibility, atoxicity and biodegradability (Bottegoni, Muzzarelli, Busilacchi, Giovannini, & Gigante, 2014; Busilacchi, Gigante, Mattioli-Belmonte, & Muzzarelli, 2013; Muzzarelli, 2009). Solubilisation of chitosan occurs in acidic aqueous medium by protonation of the $-NH_2$ functional group present on the C-2 position of the D-glucosamine repeating unit. This makes chitosan the only pseudo-natural polymer which can be applied as solution, film, fibers as well as in hydrogel form (Rinaudo, 2006; Illum, 1998). Chitosan hydrogel, the most commonly used form of chitosan can be prepared by crosslinking with glycerol in an acidic medium (Chowdhury, Gogoi, & Majumdar, 2012). Hydrogel is a three dimensional network structure of polymer which can entrap water without losing their network structure (Kiuchi, Kai, & Inoue, 2008). Kiuchi et al. reported preparation of chitosan hydrogel film cross-linked with DiepoxyPoly(ethylene glycol) with improved mechanical and swelling behavior compared to the chitosan hydrogel film cross-linked with poly(ethylene glycol) (Kiuchi et al., 2008). Khan et al. demonstrated the fabrication of improved nanocrystalline cellulose reinforced chitosan based nanocomposite films (Khan et al., 2012). So, this polymer has been used in past tuning its properties via fabrication of nanocomposites.

There are reports of using different nanomaterials like gold, silver, carbon nanotube etc. for the preparation of chitosan hydrogel nanocomposite. Recently carbon quantum dots also known as carbon dots (CDs) having sizes below 10 nm have emerged as the most alternative fluorescent nanoprobe (Qian et al., 2014) due to their easy availability, cost-effectiveness, thermal stability and relatively non-cytotoxic nature (De, Voit & Karak, 2013). Many new carbon sources for preparation of carbon dots are continuously reported since its first report by Sun et al. (2006). Sahu et al. showed carbon dots prepared from hydrothermal treatment of orange juice (Sahu, Bhhera, Maiti & Mahapatra, 2012). Zhang et al. demonstrated the preparation of fluorescent CDs directly via simple hydrothermal method using bovine serum albumin (BSA) as a carbon source in the presence of surface passivating agent (Zhang, Hao, Zhang, Zhang & Tang, 2012). Recently Hsu, Shih, Lee & Chang, (2012) showed a simple method for the preparation of carbon dots from coffee grounds. Other methods of preparing of carbon dots from egg yolk

* Corresponding author. Tel.: +91 361 2912073; fax: +91 361 2279909.
E-mail address: devasish@iasst.gov.in (D. Chowdhury).

http://dx.doi.org/10.1016/j.carbpol.2014.08.021
0144-8617/

or egg white (Wang, Wang & Chen, 2012) and ascorbic acid (Jia, Li, & Wang, 2012) has also been reported recently. We have also demonstrated a simple and convenient strategy to prepare fluorescent carbon dots from chitosan gel and also various methods developed over the years for the preparation of carbon dots finds mention in our earlier paper (Chowdhury et al., 2012).

In this report we present a new green source "tea" as a suitable precursor for synthesis of fluorescent carbon dots. These tea carbon dots are successfully utilized in preparing a chitosan–tea carbon dots nanocomposite hydrogel film with improved physico-mechanical properties compared to that of chitosan hydrogel film cross-linked only with glycerol. Tea is one of the major agro-commercial products of India. There are three main kinds of tea produced in India: Assam tea from north-eastern part of India (state of Assam), Darjeeling tea from the foothills of the Himalayas and Nilgiri tea from southern India. In this work we have successfully prepared carbon dots from Assam tea. As per our knowledge, there is only one report of preparation of chitosan nanocomposite using carbon dots. Huang et al. reported preparation of CDs nanocomposite film for dopamine biosensing (Huang et al., 2013). Here we have focused on the preparation of a green soft but tough biocompatible hydrogel film from chitosan and tea carbon dots and its varied applicability due to possession of many important properties like UV–visible blocking, excessive swelling, thermal stability and mechanical strength.

2. Experimental

2.1. Materials

Chitosan (M.W ~ 193400, degree of deacetylation = 77.7%) obtained from Sigma Aldrich, Germany was vacuum dried before every use. Glycerol (density = 1.255 at 20 °C), glacial acetic acid and sodium hydroxide (pellets) obtained from Merck, India were used without any further purification. CTC (Crush, tear, curl) tea was purchased from Jalan Golaghat Tea Co. (P) Ltd., Assam, India.

2.2. Preparation of chitosan hydrogel film

Chitosan hydrogel was prepared by following a simple protocol. A solution of glycerol and 0.1 M acetic acid solution was prepared by mixing two parts of glycerol and three parts of acetic acid. 0.1 g of chitosan was dissolved in a 10 ml of this above mentioned solution and mechanically stirred at room temperature for 2 h to allow complete dissolution of chitosan. The whole system was then neutralized by addition of 5 N sodium hydroxide solution drop wise with continuous stirring. At the neutralization point, a white sticky gel was formed due to gelation. The prepared chitosan hydrogel was then thoroughly washed with millipore water several times to remove any unreacted monomer from the chitosan hydrogel, if present. For film casting, the chitosan hydrogel was spread onto a glass plate (75 mm × 25 mm × 1.3 mm) and dried at 65 °C in a hot air oven. Dried film was peeled off from the plate after slightly wetting it with water and finally stored in vacuum dry condition at room temperature.

2.3. Synthesis of carbon dots from tea

The commercially available Assam tea was first heated at 200° C for about 2 h, followed by grinding to powdered form and again heated at 200° C for about 8 h. The so formed black carbonized powder of tea was cooled to room temperature and stored in a glass vial. Two different dispersion mediums, viz., ethanol and 0.1 M acetic acid were used in preparation of *carbon dots* from tea. A quantity of 300 mg of the carbonized tea was dispersed in 10 mL of the dispersion medium and kept for 40 h. The dispersed medium was then centrifuged (at 10,000 rpm for 0.5 h) and the supernatant liquid containing tea *carbon dots* was collected and preserved.

2.4. Preparation of chitosan–carbon dots nanocomposite hydrogel films

Chitosan–*carbon dots* nanocomposite hydrogel films were prepared by the similar solution technique followed for chitosan hydrogel films. A 0.5, 1, 1.5 and 2 wt% tea CDs (with respect to the total weight of glycerol and chitosan) prepared in 0.1 M acetic acid was added to a mixture of 0.1 g chitosan and 4 ml (5.04 g) glycerol. We have preferably chosen *carbon dots* prepared by dispersing in 0.1 M acetic acid for synthesizing chitosan–*carbon dots* hydrogel films keeping in mind the fact that chitosan is soluble in acetic acid. The resulting solutions were then mechanically stirred at room temperature for 2 h followed by neutralization of the system by adding 5 N NaOH. The hydrogels were then washed with millipore water for several times to remove unreacted monomers and casted on glass plates followed by drying at 65°C. The dried films were peeled off by wetting them with water and stored in vacuum at room temperature. The four chitosan-CDs nanocomposite hydrogel films thus prepared from 0, 0.5, 1, 1.5 and 2 wt% tea CDs were named as CH, CH-CD1, CH-CD2, CH-CD3, CH-CD4, respectively.

2.5. UV–Visible spectroscopy study of chitosan and chitosan–carbon dots nanocomposite hydrogel films

To analyse the UV–visible blocking ability, the hydrogel films were studied through UV–visible spectroscopy. The chitosan films and different nanocomposite hydrogel films (i.e., CH-CD1, CH-CD2, CH-CD3 and CH-CD4) were cut off into equal sizes (~1 × 2 cm^2) and scanned through a range of 190–800 nm wavelength in reflectance mode.

2.6. Thermal analysis

Any change in the thermal behavior of the hydrogel film on incorporation of tea carbon dots were systematically studied from thermogravimetric analysis (TGA). 5–10 mg of each hydrogel film was used for TGA under nitrogen flow.

2.7. Tensile strength (TS) and Elongation at break (E) of chitosan and chitosan- carbon dots nanocomposite hydrogel films

Mechanical properties of the hydrogel films were studied determining their tensile strength (TS) and elongation at break (E) following standard ASTM D882-91 procedure. The testing was done on Universal Testing Machine using a 100 Kg load cell at a speed of 10 mm/min. TS was measured in MPa unit which denotes the maximum force (N) per unit cross sectional area (mm^2) required to break the sample. E given here is the percent ratio of the length of the sample film at the maximum force to the original length.

2.8. Swelling study

To study the swelling behavior gravimetrically, the hydrogel films (thickness ~ 0.1 mm) were cut into equal sizes (10 × 10 mm^2) and dried in a vacuum oven overnight. Each hydrogel film of CH, CH-CD1, CH-CD2, CH-CD3 and CH-CD4 were then weighed and kept immersed in 10 mL of millipore water at room temperature for 24 h. The hydrogel films were then taken out and dried on filter paper to ensure complete removal of surface water from the hydrogel films and weighed again. Swelling ratio was determined according to the following formula:

$$\text{Swelling ratio}\,(\%) = [(W_s - W_d)/W_d] \times 100\%$$

where, W_s and W_d are weight of the swollen and dried samples respectively.

2.9. Wettability of hydrogel films

The static contact angles of the hydrogel films were measured using Contact Angle Analyzer to study the wettability of the hydrogel films. Millipore water of approximately 10 μL was dropped onto the surface of each hydrogel films and contact angle was measured. Five concurrent readings were taken for each hydrogel film and their mean is then plotted.

2.10. Characterization

The chitosan and chitosan–*carbon dots* hydrogel films were characterized by Fourier transform infrared spectrometer (Nicolet 6700 FT-IR) to investigate the chemical changes in film structure before and after treatment with tea *carbon dots*. Spectra were obtained in transmission mode from samples in KBr pellets in the range of 400–4000 cm^{-1} over 32 scans. UV-visible studies were carried out on chitosan and chitosan–*carbon dots* nanocomposite films in Shimadzu UV Spectrophotometer-UV 2600 with integrated sphere set-up. The TGA thermograms were recorded in Perkin Elmer 4000 and were done in the range of 35–800 °C at a heating rate of 10° C/min and with nitrogen flow rate of 20 ml/min. The mechanical properties of the hydrogel films were tested on Universal Testing Machine (Kalpak Instruments and Controls, Pune, 5 kN capacity). The static contact angles of the hydrogel films were measured using Contact Angle Analyzer of model DSA30, KRŰSS, Germany. The photoluminescence (PL) intensity measurements were done in Varian Cary Eclipes, Agilent spectrofluorometer. Size distribution and zeta potential studies were done using Malvern Zetasizer NanoZS 90. Surface morphology of the prepared hydrogel films were studied by scanning electron microscope (Carl Zeiss Supra 55). We also studied the distribution of carbon dots in the polymer hydrogel matrix with the help of a florescent microscope (LEICA DMI 3000 B).

3. Results and discussions

Chitosan and chitosan–carbon dots nanocomposite hydrogel films were successfully prepared by film casting method as described in the experimental section. We have used commercially available "Assam tea" as carbon source for the first time for preparing fluorescent carbon dots in two dispersion medium, viz., ethanol and 0.1 M acetic acid. Tea which is abundant in eastern part of India was used as a green and cost-effective material in preparing carbon dots.

Fig. 1A shows the schematic representation of the protocol used in preparing carbon dots from tea and Fig. 1B shows the representative Scanning Electron Microscope (SEM) image of carbon dots obtained from tea. The SEM image clearly depicted that it is possible to get nano-sized particle from tea. Dynamic Light Scattering (DLS) study was also done for the carbon dots prepared from Tea. Fig. 1C shows a typical DLS histogram of the sizes of the carbon dots obtained from tea. The average size was determined to be 2.7 nm. The zeta potential of prepared carbon dots was found to be −229 mV indicating the negative charge on the carbon dots. Tea consists of a host of chemicals like polyphenols, flavones, polyphenolic acids, carotenoids etc. So, it seems that any carbon containing material present in tea can be source of carbon dots.

Fig. 2A shows the photoluminescence (PL) emission spectra of carbon dots prepared by dispersing tea in 0.1 M acetic acid excited at different wavelength. It was observed that with increase in the excitation wavelength from 380 nm to 500 nm, the emission of

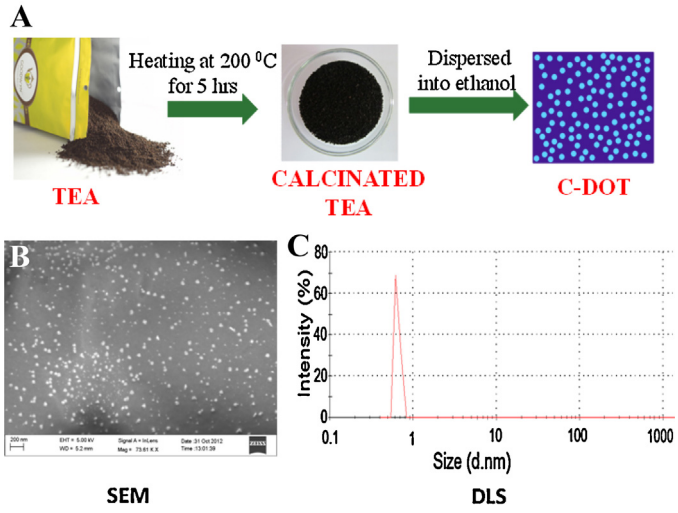

Fig. 1. (A) Schematic representation of the process involved in preparing CDs from tea (B) SEM image, and (C) DLS particle size distribution of carbon dots obtained from tea.

carbon dots gradually shifted to higher wavelengths accompanied with decreased fluorescence intensity. This red shift in the emission of carbon dots has also been reported previously (Jaiswal, Ghosh, & Chattopadhyay, 2012). It was observed that when carbon dots excited at 380, 400, 420, 440, 460, 480 and 500 nm resulted in emission at 468, 481, 506, 516, 530, 537 and 554 nm, respectively. It is believed that PL emission is consequence of both the quantum size effect and surface defects (Chowdhury et al., 2012).

Fig. 2B shows a comparative PL spectral plot of carbon dots prepared by dispersing in 0.1 M acetic acid and ethanol when excited at 380 nm. It is clear from the spectrum that when carbon dots was prepared by dispersing in 0.1 M acetic acid high intensity PL peak was obtained in comparison to when prepared by dispersing in ethanol. Also, a blue shift in emission (to 459 nm) was observed in carbon dots dispersed in ethanol compared to 468 nm emission of carbon dots dispersed in 0.1 M acetic acid. So, we prepared the chitosan–carbon dots nanocomposite in acetic acid medium.

Fig. 3 shows a schematic representation of the protocol followed for the preparation of chitosan–carbon dots nanocomposite films. A photograph of the prepared chitosan–carbon dots hydrogel film is also shown in the scheme. As demonstrated in the scheme, the positively charged $-NH_3^+$ groups of chitosan contribute to hydrogen bonding when electrostatically interact with predominant —OH groups of tea carbon dots. Further evidence comes from zeta potential values, which showed that while chitosan with $-NH_3^+$ groups are positively charged (+35 mV), CDs prepared from tea is negatively charged (−229 mV). Also, there might be extensive hydrogen bonding between –OH group on carbon dots and $-CH_2OH$ group of chitosan and —OH of glycerol. We want to add here that we have prepared carbon dots from citric acid (Baruah, Deka & Chowdhury, 2014) another carbon source other than tea to check the exclusive role of tea in the hydrogel film, if any (Fig. S1, electronic supplementary material). Interestingly, it was observed that carbon dots from citric acid showed a high positive zeta potential value (112 mV). Also, the hydrogel film prepared from chitosan–citric acid carbon dots nanocomposite following the same protocol used for preparation of chitosan–tea carbon dots nanocomposite film was found to be very fragile (Fig. S2, electronic supplementary material). Thus, we can conclude that negative zeta potential value of tea CDs might be one of the key factor of strong electrostatic interaction in the prepared chitosan–carbon dot nanocomposite films.

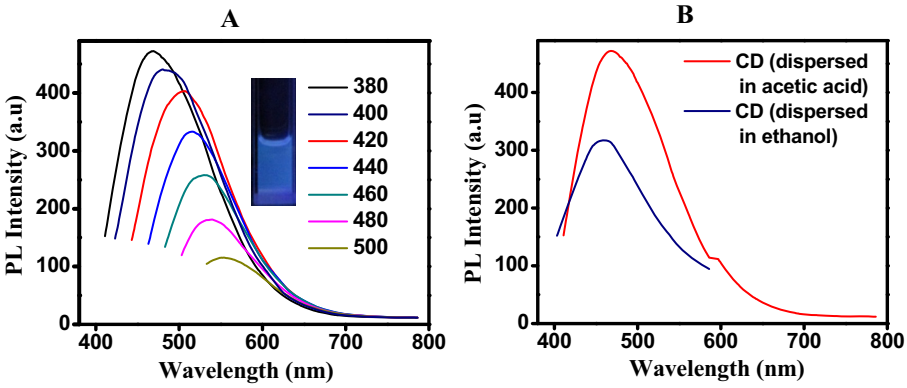

Fig. 2. (A) Photoluminescence emission obtained with progressively longer excitation wavelengths from 380–500 nm of CDs obtained from tea dispersed in 0.1 M acetic acid. Inset: photograph of cuvette containing the carbon dots viewed under illumination with UV lamp. (B) Comparison of photoluminescence emission obtained with excitation wavelength at 380 nm of carbon dots dispersed in ethanol and 0.1 M acetic acid.

A FTIR study of CH, CH-CD1 hydrogel films and tea carbon dots were done to validate all these electrostatic interactions between carbon dots and chitosan (Fig. 4). The broadening of peak around 3400 cm^{-1} in FTIR spectra of chitosan–carbon dots in comparison to that of chitosan hydrogel film indicates hydrogen bonding between —OH groups of chitosan, glycerol and carbon dots. The peak at 1644 cm^{-1} of CH is shifted to 1648 cm^{-1} in CH-CD1 due to increased C=C stretching. The C—N stretching frequency contributes to peak 1350–1080 cm^{-1}. The aromatic out of plane C—H bending is contributing to peak around 900–669 cm^{-1}.

UV–visible studies were carried out on chitosan and chitosan–carbon dots nanocomposite film and shown in Fig. 5A. It is evident from the spectra that as the content of carbon dots were increased in the nanocomposite film the transmittance decreased and is almost same in the wavelength range of 300–600 nm. The % transmittance reduced to 20% for CH-CD4 nanocomposite film in the wavelength range of 300–600 nm. The absorption in the UV–visible region is usual, easy to interpret and is due to the $n \rightarrow \pi^*$ transition of the C=O bond. In chitosan- carbon dots nanocomposite hydrogel films, a large number of highly conjugated aromatic structures from tea CDs is also present which contributes to $\pi \rightarrow \pi^*$ transition. Thus, there is decrease in HOMO–LUMO energy gap, which causes a bathochromic shift resulting in higher absorption intensity towards visible region (De et al., 2013; Matsumi, Naka, Chujo, 1998). As a consequence chitosan–carbon dots nanocomposite films were less transparent in the wavelength region of 300–600 nm when compared with chitosan hydrogel films.

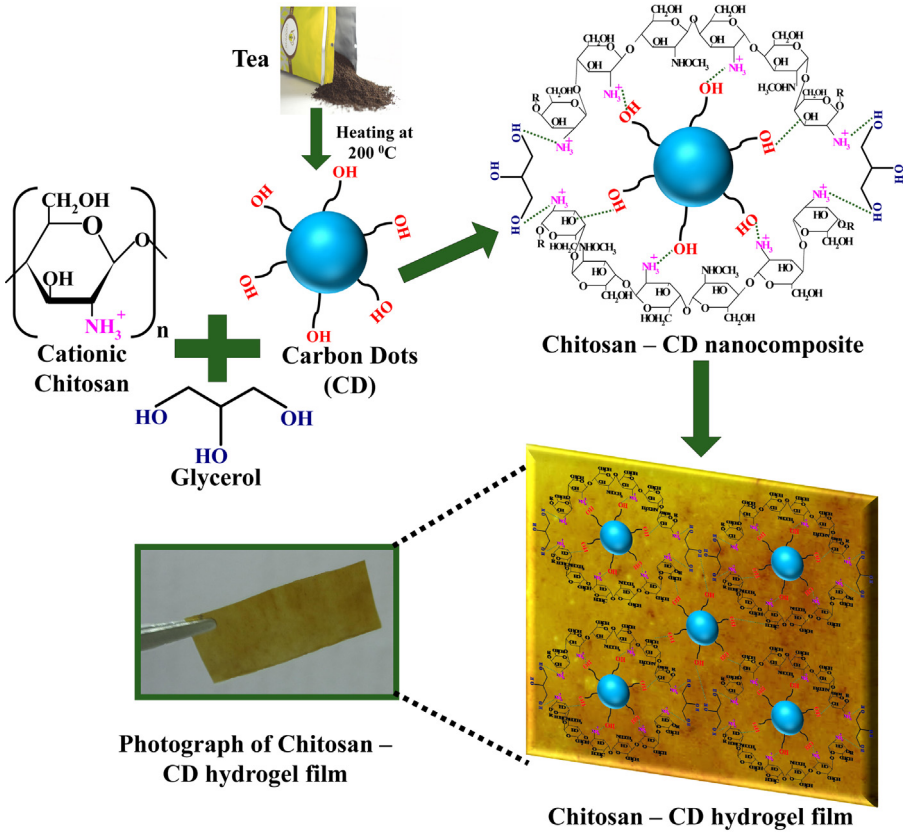

Fig. 3. The schematic representation of the protocol followed in preparation of Chitosan–Carbon dots nanocomposite film.

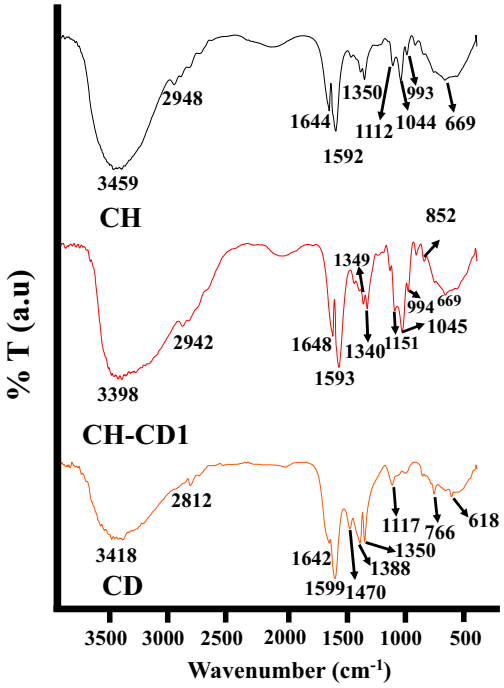

Fig. 4. FTIR spectrum of carbon dots prepared from tea, CH and CH-CD1 nanocomposite films.

X-ray diffraction (XRD) study of CH and CH-CD1, CH-CD2, CH-CD3 and CH-CD4 nanocomposite films are shown in Fig. 5B. Peak at 20.3° in the diffractogram of chitosan hydrogel film indicated the high degree of crystallinity of chitosan film. However, the peaks were also present in all the chitosan–carbon dots nanocomposite films confirming the retention of crystallinity after incorporation of carbon dots.

Thermal stability study was carried out on chitosan and chitosan–carbon dots nanocomposite films in order to decipher the role of carbon dots prepared from tea in thermal stability of the chitosan–carbon dots nanocomposite films. Fig. 6A shows the thermograms of chitosan and chitosan–carbon dots nanocomposite films. It is interesting to note that at 250 °C, there was about 42% weight loss observed in CH, but only 21% was observed in CH-CD1, which gradually decreased further to 19%, 16% and 13% in CH-CD2, CH-CD3 and CH-CD4, respectively. It was also evident from the thermograms that the chitosan and chitosan–carbon dots nanocomposite films showed two stages degradation. In CH hydrogel film, the first stage degradation occurred from 180 °C to 330 °C, which was attributed due to degradation of side chain fragments of chitosan and glycerol structure. On the other hand, the first stage degradation of CH-CD1 was shifted to about 85 °C towards high temperature, which in turn interestingly shifted up to as high as 100 °C towards higher temperature in CH-CD4. This extraordinary thermal stability of chitosan–carbon dots nanocomposite films was also due to the presence a large number of aromatic structures present in carbon dots prepared from tea acting as a thermal barrier and hence preventing degradation. The second stage degradation of all the hydrogel films started from about 500 °C, which was mainly due to breakdown of the aromatic moieties in the nanocomposite films.

The wettability of a solid surface generally depends on its chemical composition and topology. Fig. 6B shows the advancing contact angle of chitosan and chitosan–carbon dots nanocompsite hydrogel films. In chitosan–carbon dots nanocomposite films, as carbon dots were obtained from tea, which contains mainly polyphenols, i.e., —OH group containing aromatic compounds, on incorporation of carbon dots to chitosan the density of hydrophobic aromatic groups increased on the surface of the films. Hence, the advancing contact angle increased from 64.95–88.75° as obtained for CH-CD3. However CH-CD4 showed lower advancing contact angle of 78.02°. Increasing surface smoothness of the nanocomposite hydrogel films evident from the SEM images (Fig. 7B also contributed to hydophobicity (Voronov, Papavassiliou, Lee, 2008). Fig. 7B shows the representative scanning electron microscope (SEM) images of the chitosan film and chitosan–carbon dots nanocomposite hydrogel film. The SEM images clearly showed the change in surface morphology before and after incorporation of carbon dots into the chitosan hydrogel matrix. The smoothness of the chitosan–carbon dots films with increasing carbon dots was due to property of carbon dots to act as filler thus contributing to the smooth film surface (Njuguna, Pielichowski, & Desai, 2008).

A systematic swelling study was also undertaken in chitosan and chitosan–carbon dots nanocomposite films. It was observed that when kept in water for 24 h, chitosan hydrogel film showed a swelling ratio (SR) of 52.2%, which increased up to 82.2% in CH-CD1. The SR was then again found to decrease to a value of 57%, 54.0% and 13.1% in CH-CD2, CH-CD3 and CH-CD4, respectively. The reason for higher SR value for CH-CD1 may be due to optimum localization of the crosslink density thereby increasing the porosity in comparison to CH hydrogel film. However CH-CD2, CH-CD3 and CH-CD4 due to presence of high concentration of carbon dots than the optimum value the localization of the crosslink density no longer existed. Instead high amount of crosslink density led to a minimal water absorption in CH-CD2, CH-CD3 and CH-CD4 hydrogel films (Chen et al., 2008; Kasgöz, Durmus, Kasgöz, 2008).

The mechanical properties like mechanical strength and elongation at break was also investigated for chitosan and chitosan–carbon dots hydrogel films. Tensile strength (TS) of CH film was determined to be 5.1 MPa as shown in Fig. 8A. The TS increased considerably to 18.6 MPa in case of CH-CD1 (comparable

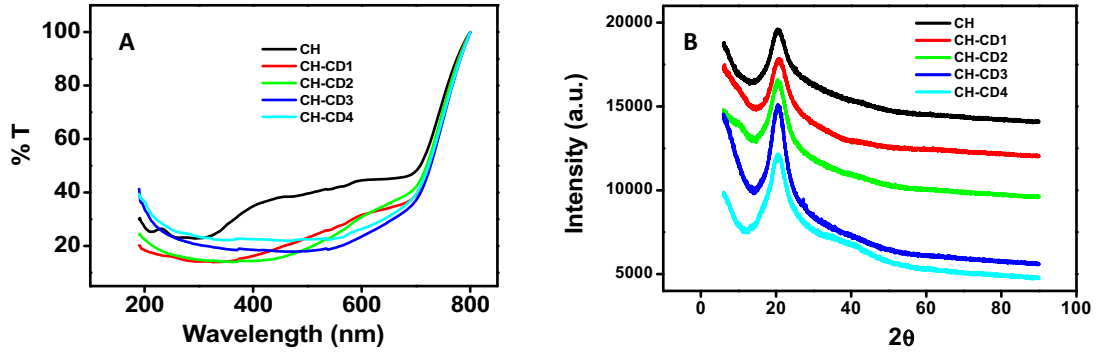

Fig. 5. (A) UV–visible spectra and (B) XRD graphs of CH, CH-CD1, CH-CD2, CH-CD3 and CH-CD4 nanocomposite films.

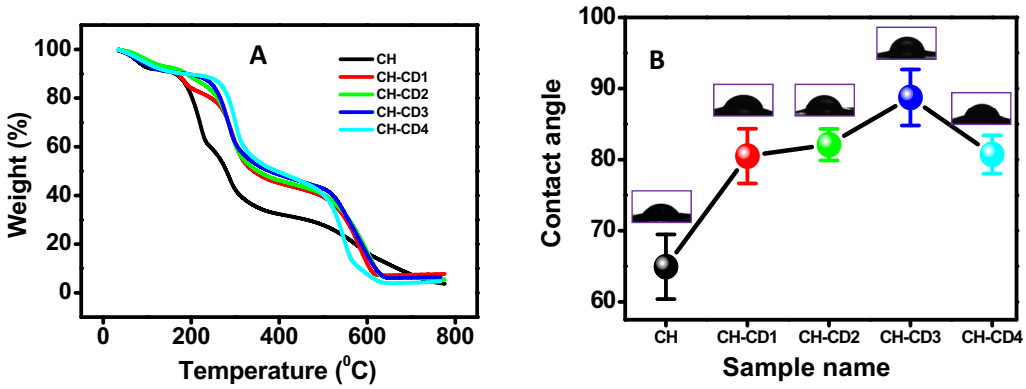

Fig. 6. (A) Thermogravimetric analysis (TGA) graph and (B) Dynamic Contact angle measurements of CH, CH-CD1, CH-CD2, CH-CD3 and CH-CD4 nanocomposite films. Inset: photographs of the drop bubble on the respective hydrogel.

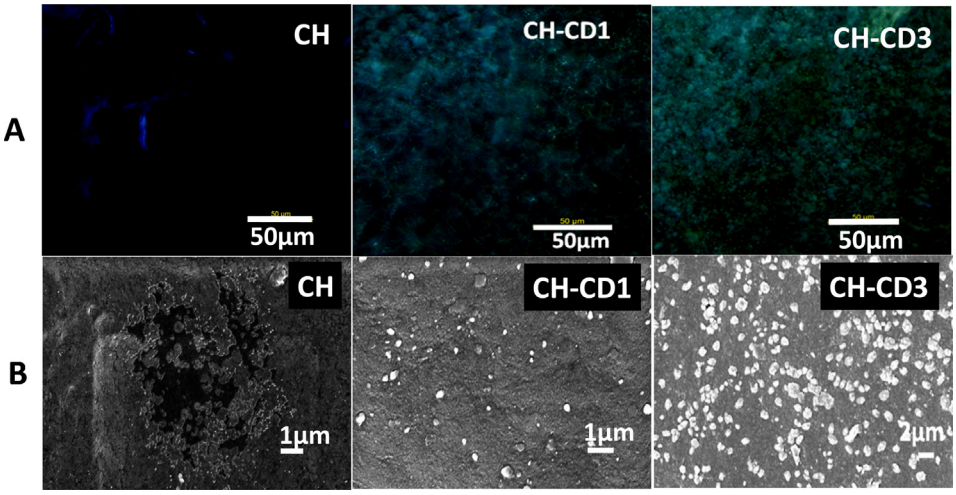

Fig. 7. Representative (A) fluorescent microscopic images and (B) scanning electron microscope (SEM) images of chitosan hydrogel (CH) and chitosan hydrogel nanocomposite (CH-CD1, CH-CD2) films.

to that of low density polyethylene). However the tensile strength decreased on further increase in carbon dots as shown by CH-CD2, CH-CD3 and CH-CD4. The average TS values were 14.7, 12.9, 8.3 MPa in CH-CD2, CH-CD3 and CH-CD4 respectively. The increased mechanical strength of the chitosan–carbon dots nanocomposite films compared to that of the chitosan hydrogel film was attributed by the strong electrostatic interaction between the polymer hydrogel matrix and stiff carbon dots. However with increase in the concentration of the carbon-dots some aggregation of the same in the polymer matrix may occurred which was evident from the SEM and fluorescent microscopic images (Fig. 7). This probably led to decrease in tensile strength value in the chitosan- carbon dots nanocomposite films with increase in carbon dots concentration (De et al., 2013). Tensile strength (TS) of these hydrogel films were found to be comparatively less than that of already reported other chitosan films. This was mainly because the hydrogel film

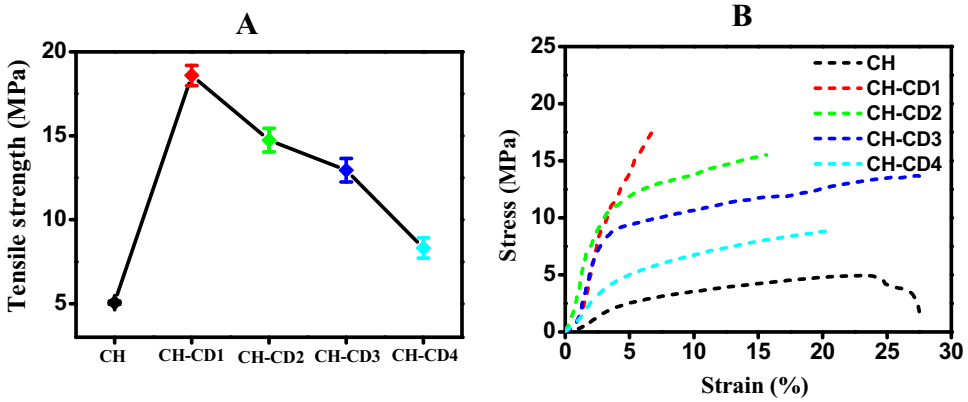

Fig. 8. (A) Comparison of Tensile strength, and (B) Stress and strain curve of CH, CH-CD1, CH-CD2, CH-CD3 and CH-CD4 nanocomposite films.

Table 1
Listed tensile strength in MPa and % elongation at break of chitosan and chitosan-carbon dot nanocomposite hydrogel films.

Sample name	Tensile strength (MPa)	Elongation at break (%)
CH	5.057	27.65
CH-CD1	18.595	6.55
CH-CD2	14.74	17.8
CH-CD3	12.95	26.35
CH-CD4	8.32	20.85

was found to have low crosslinking density with network like porous structure. But this approach on the other hand facilitated to prepare a soft but tough (as indicated by the stress-strain curves; Fig. 8B) biocompatible film which may potentially be used in various biomedical applications.

Another property that was studied was elongation at break (Table 1) which was found to decrease on incorporation of carbon dots prepared from tea into the hydrogel matrix. This may be attributed due to increasing crosslink density as stronger electrostatic interaction occurring in chitosan–carbon dots hydrogel matrix which allowed lesser flexibility of the hydrogel matrix (Xu, Ren, Hanna 2006). However increase in carbon dots concentration improved the toughness of the nanocomposite films which was measured by the area under the stress strain curve (Fig. 8B). This can be related to the stiffening effect of the carbon dots, which has aromatic carbonized core structure. So, the toughness of the nanocomposite films increased up to near about 285% compared to the chitosan hydrogel film on incorporation of 1.5% carbon dots. As in case of the previous properties the toughness of the hydrogel films also showed a decrease for CH-CD4 nanocomposite film which may be due to overloading or agglomeration of carbon dots at higher concentration (De, Voit & Karak, 2013; Shah, Maiti, Siang, Batt, Giannelis, 2005).

4. Conclusion

In conclusion, we have reported herein fabrication of a soft but tough chitosan–carbon dots nanocomposite hydrogel film possessing interesting properties. The carbon dots used in making the nanocomposite was prepared from a new green source “tea”. The basic criteria for the preparation of such hydrogel films were the successful electrostatic interaction between positive charge on chitosan and negative charge on carbon dots. These electrostatic interactions helped the chitosan–carbon dots films to have excellent superior properties like UV–visible blocking, thermal stability and mechanical strength in comparison to chitosan hydrogel films. The % transmittance in the wavelength range of 300–600 nm showed reduction up to 20% for CH-CD4 in comparison to CH hydrogel film. The Tensile strength (TS) of CH-CD1 nanocomposite film increased considerably to 18.6 MPa in comparison to CH hydrogel film (5.1 MPa). Also, the contact angle values increased from 64.95° for CH films to 88.75° for CH-CD3 nanocomposite film suggesting increase in hydrophobicity of the nanocomposite hydrogel films. Thus simply tuning of the concentration of tea carbon dots in the nanocomposite hydrogel films offers avenues to develop hydrogel films of interesting and desired properties. This also leads to fabrication of such biocompatible and green chitosan–carbon dots nanocomposite films for applications in biomedical and industrial fields.

Acknowledgment

The authors would like to thank Council of Scientific and Industrial Research (CSIR), New Delhi for the project No. 01(2488)/11/EMR-II), All India Council For Technical Education, New Delhi for the project 8023/RID/RPS-3/(NER)2011-12, Science and Engineering Research Board (SERB), New Delhi for project grant SR/S1/PC/0058/2010 and SB/S1/PC-69/2012. Authors would like to acknowledge help from Dr. Tridib Sarma for SEM images and Dr. Nandana Bhardwaj for fluorescent microscopy. AK thanks IASST for fellowship. NG thanks CSIR, New Delhi for fellowship.

Appendix A. Supplementary data

Supplementary data associated with this article can be found, in the online version, at http://dx.doi.org/10.1016/j.carbpol.2014.08.021.

References

Baruah, U., Deka, M. J., & Chowdhury, D. (2014). Reversible On/Off Switching of fluorescence via esterification of carbon dots. *RSC Advances*, *4*, 36917–36922.
Bottegoni, C., Muzzarelli, R. A. A., Busilacchi, A., Giovannini, F., & Gigante, A. (2014). Oral chondroprotection with nutraceuticals made of chondroitin sulphate plus glucosamine sulphate in osteoarthritis. *Carbohydrate Polymers*, *109*, 126–138.
Busilacchi, A., Gigante, A., Mattioli-Belmonte, M., & Muzzarelli, R. A. A. (2013). Chitosan stabilizes platelet growth factors and modulates stem cell differentiation toward tissue regeneration. *Carbohydrate Polymers*, *98*, 665–676.
Chen, P. H., Kuo, T. Y., Liu, F. H., Hwang, Y. H., Ho, M. H., Wang, D. M., et al. (2008). Use of dicarboxylic acids to improve and diversify the material properties of porous chitosan membranes. *Journal of Agriculture and Food Chemistry*, *56*, 9015–9021.
Chowdhury, D., Gogoi, N., & Majumdar, G. (2012). Fluorescent CDs obtained from chitosan gel. *RSC Advances*, *2*, 12156–12159.
De, B., Voit, B., & Karak, N. (2013). Transparent luminescent hyperbranched epoxy/carbon oxide dot nanocomposites with outstanding toughness and ductility. *ACS Applied Materials & Interfaces*, *5*, 10027–10034.
Hsu, P. C., Shih, Z. Y., Lee, C. H., & Chang, H. T. (2012). Synthesis and analytical applications of photoluminescent carbon nanodots. *Green Chemistry*, *14*, 917–920.
Huang, Q., Hu, S., Zhang, H., Chen, J., He, Y., & Li, F. (2013). CDs and chitosan composite film based biosensor for the sensitive and selective determination of dopamine. *Analyst*, *138*, 5417–5423.
Illum, L. (1998). Chitosan and its use as a pharmaceutical excipient. *Pharmaceutical Research*, *15*, 1326–1331.
Jia, X., Li, J., & Wang, E. (2012). One-pot green synthesis of optically pH-sensitive CDs with upconversion luminescence. *Nanoscale*, *4*, 5572–5575.
Jaiswal, A., Ghosh, S. S., & Chattopadhyay, A. (2012). One step synthesis of C-dots by microwave mediated caramelization of poly (ethylene glycol). *Chemical Communication*, *48*, 407–409.
Kasgöz, H., Durmus, A., & Kasgöz, A. (2008). Enhanced swelling and adsorption properties of AAm-AMPSNa/clay hydrogel nanocomposites for heavy metal ion removal. *Polymers for Advanced Technologies.*, *19*, 213–220.
Khan, A., Khan, R. A., Salmieri, S., Tien, C. L., Riedl, B., Bouchard, J., et al. (2012). Mechanical and barrier properties of nanocrystalline cellulose reinforced chitosan based nanocomposite films. *Carbohydrate Polymers*, *90*, 1601–1608.
Kiuchi, H., Kai, W., & Inoue, Y. (2008). Preparation and characterization of poly (ethylene glycol) crosslinked chitosan films. *Journal of Applied Polymer Science*, *107*, 3823–3830.
Matsumi, N., Naka, K., & Chujo, Y. (1998). Extension of ϖ-conjugation length via the vacant p-orbital of the boron atom. Synthesis of novel electron deficient ϖ-conjugated systems by hydroboration polymerization and their blue light emission. *Journal of American Chemical Society*, *120*, 5112–5113.
Muzzarelli, R. A. A., Boudrant, J., Meyer, D., Manno, N., DeMarchis, M., & Paoletti, M. G. (2012). A tribute to Henri Braconnot, precursor of the carbohydrate polymers science, on the chitin bicentennial. *Carbohydrate Polymers*, *87*, 995–1012.
Muzzarelli, R. A. A. (2010). Chitins and chitosans as immunoadjuvants and non-allergenic drug carriers. *Marine Drugs*, *8*, 292–312. Open access
Muzzarelli, R. A. A. (2012). Nanochitins and nanochitosans, paving the way to eco-friendly and energy-saving exploitation of marine resources. *Polymer Science: A Comprehensive Reference*, *10*, 153–164.
Muzzarelli, R. A. A. (2009). Chitins and chitosans for the repair of wounded skin, nerve, cartilage and bone. *Carbohydrate Polymers*, *76*, 167–182.
Njuguna, J., Pielichowski, K., & Desai, S. (2008). Nanofiller-reinforced polymer nanocomposites. *Polymers for Advanced Technologies*, *19*, 947–959.
Qian, J., Chen, J. T., Ruan, S. B., Shen, S., He, Q., Jiang, X. G., et al. (2014). Preparation and biological evaluation of photoluminescent carbonaceous nanospheres. *Journal of Colloid and Interface Science*, *429*, 77–82.
Rinaudo, M. (2006). Chitin and chitosan: Properties and applications. *Progress in Polymer Science*, *31*, 603–632.
Sun, Y. P., Zhou, B., Lin, Y., Wang, W., Fernando, K. A. S., Pathak, P., et al. (2006). Quantum-sized CDs for bright and colorful photoluminescence. *Journal of American Chemical Society*, *128*, 7756–7757.
Sahu, S., Behera, B., Maiti, T. K., & Mohapatra, S. (2012). Simple one-step synthesis of highly luminescent CDs from orange juice: Application as excellent bio-imaging agents. *Chemical Communication*, *48*, 8835–8837.
Shah, D., Maiti, P., Siang, D. D., Batt, C., & Giannelis, A. E. P. (2005). Effect of nanoparticle mobility on toughness of polymer nanocomposites. *Advanced Materials*, *17*, 525–528.

Voronov, R. S., Papavassiliou, D. V., & Lee, L. L. (2008). Review of fluid slip over superhydrophobic surfaces and its dependence on the contact angle. *Industrial & Engineering Chemistry Research*, *47*, 2455–2477.

Wang, J., Wang, C. F., & Chen, S. (2012). Amphiphilic egg-derived CDs: Rapid plasma fabrication, pyrolysis process, and multicolor printing patterns. *Angewandte Chemie International Edition*, *51*, 9297–9301.

Xu, Y., Ren, X., & Hanna, M. A. (2006). Chitosan/clay nanocomposite film preparation and characterization. *Journal of Applied Polymer Science*, *99*, 1684–1691.

Zhang, z., Hao, J., Zhang, J., Zhang, B., & Tang, J. (2012). Protein as the source for synthesizing fluorescent CDs by a one-pot hydrothermal route. *RSC Advances*, *2*, 8599–8601.